

## Ribosome Rescue Inhibitors Kill Actively Growing and Non-replicating Persister *Mycobacterium tuberculosis* Cells

John N Alumasa, Paolo Solano Manzanillo, Nicholas D. Peterson, Tricia Lundrigan, Anthony D. Baughn, Jeffery S. Cox, and Kenneth C. Keiler

*ACS Infect. Dis.*, **Just Accepted Manuscript** • DOI: 10.1021/acsinfecdis.7b00028 • Publication Date (Web): 01 Aug 2017

Downloaded from <http://pubs.acs.org> on August 2, 2017

### Just Accepted

“Just Accepted” manuscripts have been peer-reviewed and accepted for publication. They are posted online prior to technical editing, formatting for publication and author proofing. The American Chemical Society provides “Just Accepted” as a free service to the research community to expedite the dissemination of scientific material as soon as possible after acceptance. “Just Accepted” manuscripts appear in full in PDF format accompanied by an HTML abstract. “Just Accepted” manuscripts have been fully peer reviewed, but should not be considered the official version of record. They are accessible to all readers and citable by the Digital Object Identifier (DOI®). “Just Accepted” is an optional service offered to authors. Therefore, the “Just Accepted” Web site may not include all articles that will be published in the journal. After a manuscript is technically edited and formatted, it will be removed from the “Just Accepted” Web site and published as an ASAP article. Note that technical editing may introduce minor changes to the manuscript text and/or graphics which could affect content, and all legal disclaimers and ethical guidelines that apply to the journal pertain. ACS cannot be held responsible for errors or consequences arising from the use of information contained in these “Just Accepted” manuscripts.



1  
2  
3  
4  
5  
6  
7  
8 **Ribosome Rescue Inhibitors Kill Actively Growing and Non-**  
9 **replicating Persister *Mycobacterium tuberculosis* Cells**  
10  
11  
12  
13  
14  
15  
16  
17

18 John N. Alumasa,<sup>†</sup> Paulo S. Manzanillo,<sup>§</sup> Nicholas D. Peterson,<sup>¶</sup> Tricia Lundrigan,<sup>§</sup>  
19 Anthony D. Baughn,<sup>¶</sup> Jeffery S. Cox,<sup>§</sup> Kenneth C. Keiler.<sup>\*,†</sup>  
20  
21  
22  
23  
24  
25  
26

27 <sup>†</sup>401 Althouse Laboratory, Department of Biochemistry and Molecular Biology, The  
28 Pennsylvania State University, University Park, PA 16802.  
29  
30

31 <sup>§</sup>375E Li Ka Shing Center, Department of Molecular and Cell Biology, University of  
32 California, Berkeley, #3370, Berkeley, CA 94720.  
33  
34  
35

36 <sup>¶</sup>Department of Microbiology and Immunology, Microbiology Research Facility, Rm4-  
37 115, University of Minnesota, 689 23<sup>rd</sup> Ave SE, Minneapolis, MN 55455.  
38  
39  
40

41 \*email: kkeiler@psu.edu  
42  
43  
44  
45  
46  
47  
48  
49  
50  
51  
52  
53  
54  
55  
56  
57  
58  
59  
60

1  
2  
3 The emergence of *Mycobacterium tuberculosis* (MTB) strains that are resistant to most  
4  
5 or all available antibiotics has created a severe problem for treating tuberculosis, and  
6  
7 has spurred a quest for new antibiotic targets. Here we demonstrate that *trans*-  
8  
9 translation is essential for growth of MTB and is a viable target for development of anti-  
10  
11 tuberculosis drugs. We also show that an inhibitor of *trans*-translation, KKL-35, is  
12  
13 bactericidal against MTB under both aerobic and anoxic conditions. Biochemical  
14  
15 experiments show that this compound targets helix 89 of the 23S rRNA. *In silico*  
16  
17 molecular docking predicts a binding pocket for KKL-35 adjacent to the peptidyl-transfer  
18  
19 center in a region not targeted by conventional antibiotics. Computational solvent  
20  
21 mapping suggests that this pocket is a druggable hot spot for small molecule binding.  
22  
23 Collectively, our findings reveal a new target for anti-tuberculosis drug development and  
24  
25 provide critical insight on the mechanism of antibacterial action for KKL-35 and related  
26  
27 1,3,4-oxadiazole benzamides.  
28  
29  
30  
31  
32  
33  
34  
35  
36  
37  
38

39 **KEYWORDS:** *Mycobacterium tuberculosis*, antibiotics, 1,3,4-oxadiazoles, ribosome  
40  
41 rescue  
42  
43  
44  
45  
46  
47  
48  
49  
50  
51  
52  
53  
54  
55  
56  
57  
58  
59  
60

1  
2  
3 Over 1.8 billion people are infected with MTB worldwide, 10% of whom are predicted to  
4 develop the active disease.<sup>1</sup> These infections produce 1.5 million deaths annually.  
5  
6 Antibiotic treatment has reduced the mortality rate of MTB, but the rise of multi-drug  
7 resistant (MDR-TB) and extensively drug resistant (XDR-TB) strains has raised an  
8 urgent need for new antibiotics.<sup>2</sup> Drugs with new chemical scaffolds and new molecular  
9 targets are particularly desirable because they are less likely to be counteracted by  
10 existing resistance mechanisms in clinical strains. The *trans*-translation pathway for  
11 rescue of nonstop ribosomes presents a potential target for antibiotics because it is  
12 required for viability or virulence in many pathogens, and is not found in metazoans.<sup>3,4</sup>  
13  
14 *trans*-Translation is used to rescue ribosomes that are trapped at the 3' end of an  
15 mRNA that has no in-frame stop codon to allow termination. During *trans*-translation, a  
16 specialized RNA molecule, tmRNA, and a small protein, SmpB, recognize these  
17 nonstop translation complexes.<sup>4</sup> tmRNA acts first like a tRNA to accept the nascent  
18 polypeptide, and then a reading frame within tmRNA is inserted into the mRNA channel.  
19 Translation resumes using tmRNA as a message and terminates at a stop codon within  
20 tmRNA, releasing the ribosome and a protein with the tmRNA-encoded peptide  
21 sequence at its C terminus.<sup>4-6</sup> Multiple proteases recognize the tmRNA-encoded peptide  
22 and rapidly degrade the protein, thereby clearing both the stalled ribosome and the  
23 incomplete polypeptide.<sup>7,8</sup> Nonstop translation complexes occur frequently in bacteria  
24 because they arise both from damaged mRNAs that lack a stop codon (nonstop mRNA)  
25 and from cleavage of mRNAs before or during translation.<sup>9</sup> In some bacteria, *trans*-  
26 translation is the only mechanism known to rescue nonstop translation complexes, and  
27 both tmRNA and SmpB are essential for viability.<sup>10</sup> Other species have the ArfA or ArfB  
28  
29  
30  
31  
32  
33  
34  
35  
36  
37  
38  
39  
40  
41  
42  
43  
44  
45  
46  
47  
48  
49  
50  
51  
52  
53  
54  
55  
56  
57  
58  
59  
60

1  
2  
3 backup systems that can release ribosomes from nonstop translation complexes in the  
4 absence of *trans*-translation.<sup>11,12</sup> The MTB genome does not encode ArfA or ArfB,  
5 suggesting that *trans*-translation is likely to be essential, and therefore a good candidate  
6 for target-based drug development. Despite a report that the anti-tuberculosis drug  
7 pyrazinamide targets *trans*-translation,<sup>13</sup> careful experiments have shown that *trans*-  
8 translation is not inhibited by pyrazinamide or its active metabolite, pyrazinoic acid, *in*  
9 *vitro* or *in vivo*<sup>14</sup>. Therefore, there are currently no antibiotics that target this pathway.

## 20 21 **RESULTS and DISCUSSION**

### 22 23 24 **SmpB is essential in *M. tuberculosis***

25  
26  
27  
28  
29 To assess the importance of *trans*-translation in MTB, we first attempted to delete the  
30 genes encoding tmRNA (*ssrA*) and SmpB (*smpB*) from the MTB chromosome using  
31 allelic exchange, but we could not obtain a deletion of either gene. To rigorously  
32 determine if *trans*-translation is essential in MTB, we engineered a strain  
33 (*TetpsmpB:rTetR*) in which the expression of *smpB* at its chromosomal locus is  
34 controlled by the tet repressor (TetR), such that addition of anhydrotetracycline (ATc)  
35 shuts off SmpB production (**Fig. 1a**). *TetpsmpB:rTetR* cells grew at a similar rate to  
36 wild-type cells in the absence of ATc, but addition of ATc severely inhibited growth (**Fig.**  
37  
38  
39  
40  
41  
42  
43  
44  
45  
46  
47  
48  
49  
50  
51  
52  
53  
54  
55  
56  
57  
58  
59  
60  
**1b**). Addition of ATc had no effect on growth of wild-type cells or control strains lacking  
*tetR* (**Fig. 1b**). These data indicate that SmpB is required for growth of MTB in culture.  
This conclusion is consistent with data from saturating transposon mutagenesis screens  
that failed to recover insertions in *ssrA* or *smpB*,<sup>15</sup> and with data demonstrating that the

1  
2  
3 chromosomal copy of *ssrA* could only be deleted in the presence of an additional copy  
4  
5 of the gene.<sup>16</sup> A MTB strain deleted for *smpB* has been reported,<sup>16</sup> but whole-genome  
6  
7 sequencing of this strain showed that the *smpB* coding sequence was present (**Fig. 1c**,  
8  
9 GenBank accession numbers: SAMN05907893 and SAMN05907849). qRT-PCR to  
10  
11 detect the SmpB mRNA in this deletion strain,  $\Delta smpB::dif$ , revealed that the gene is  
12  
13 expressed (**Fig. 1d**). Taken together, these results demonstrate that *trans*-translation is  
14  
15 essential for growth in MTB.  
16  
17  
18  
19  
20

### 21 **KKL-35 kills growing and non-replicating persister cells of *M. tuberculosis***

22  
23  
24

25 KKL-35 (**Fig. 2a**) and related 1,3,4-oxadiazole benzamides, were identified by cell-  
26  
27 based screening for inhibitors of *trans*-translation, and were found to have broad-  
28  
29 spectrum antibacterial activity.<sup>17,18</sup> To assess the ability of KKL-35 to inhibit growth of  
30  
31 MTB, MIC and plating assays were performed. KKL-35 inhibited growth of MTB cultures  
32  
33 with a MIC of 1.6  $\mu\text{g/ml}$ , and plating assays showed that 8.0  $\mu\text{g/ml}$  KKL-35 killed >90%  
34  
35 of MTB cells within seven days (**Fig. 2b, c**). Tuberculosis infections can be difficult to  
36  
37 treat in part because MTB cells can enter a nonreplicating persister state in which they  
38  
39 are not sensitive to most antibiotics. We used a hypoxia persistence model<sup>19</sup> to evaluate  
40  
41 the activity of KKL-35 against nonreplicating persister bacilli. 1.6  $\mu\text{g/ml}$  KKL-35 killed  
42  
43 >90 % of nonreplicating MTB cells under these conditions, demonstrating that KKL-35  
44  
45 was equally active against nonreplicating MTB cells as it was against actively growing  
46  
47 cells (**Fig. 2d**). The observed activity against persister cells suggests that *trans*-  
48  
49 translation is required for survival in this state, and indicates that *trans*-translation  
50  
51 inhibitors may be effective against multiple physiological states of MTB during infection.  
52  
53  
54  
55  
56  
57  
58  
59  
60

Despite its potency against MTB, KKL-35 and its analogs displayed no cytotoxic activity against HeLa cells (**Table 1**) or HepG2 cells<sup>18</sup> at concentrations >20-fold MIC. The combination of significant antibiotic activity against MTB and low cytotoxic activity for KKL-35 indicates that this compound is a promising anti-tubercular agent.

### KKL-35 targets helix 89 of 23S rRNA

To determine the molecular target for KKL-35, we designed and synthesized an analog, KKL-2098, incorporating a photo-reactive azide group and a terminal alkyne moiety (**Fig. 2a, Scheme 1**). The MICs for KKL-2098 against *Mycobacterium smegmatis* and other bacterial species were similar to those for KKL-35 (**Table 1**). The similarity in activity suggests that the structural modifications in this analog did not significantly alter antibiotic properties or target binding of the compound. We therefore used *M. smegmatis* for the KKL-35 target identification. Intracellular photo-affinity labeling followed by click bioconjugation was used in the molecular target identification process (**Fig. 3**).<sup>20,21</sup>

**Table 1. Comparison of the antibacterial activity for KKL-35, KKL-40 and KKL-2098.**

Compound ID	MIC <sup>a</sup> (μg/ml)					Cytotoxicity <sup>g</sup>	
	<i>B. anthracis</i> <sup>b</sup>	<i>E. coli</i> Δ <i>tolC</i> <sup>c</sup>	<i>S. flexneri</i> <sup>d</sup>	<i>M. smegmatis</i> <sup>e</sup>	MTB <sup>f</sup>	HeLa (μg/ml)	
KKL-35	0.3 (0.1)	0.5 (0.1)	1.6 (0)	0.4 (0)	1.6 (0)	> 31.8	
KKL-40	0.1 (0)	0.2 (0)	1.8 (0)	0.3 (0)	1.8 (0)	> 31.8	
KKL-2098	0.3 (0.1)	0.5 (0.1)	1.7 (0)	0.4 (0)	ND	ND	

<sup>a</sup>Data are averages from three independent assays each performed in triplicate (SD);

<sup>b</sup>Sterne strain 34F2; <sup>c</sup>Strain MG1655; <sup>d</sup>Strain 2a 2457T; <sup>e</sup>Strain mc<sup>2</sup>155 (ATCC

1  
2  
3 700084); <sup>f</sup>Erdman strain; <sup>g</sup>From > 3 independent determinations; <sup>b-e</sup>MICs for KKL-35 and  
4  
5 KKL-40 for these strains have been previously reported.<sup>17</sup>; ND: not determined.  
6  
7

8  
9  
10 To facilitate isolation and visualization of the target we also synthesized a tri-functional  
11 probe, KKL-2107 (**Fig. 2a, Scheme 2**), that incorporated an azide group, an affinity  
12 conjugate and a fluorescent moiety. The target was identified by incubating KKL-2098  
13 with growing *M. smegmatis* cells and irradiating the culture with UV light to initiate  
14 cross-linking (**Fig. 3**). Following cross-linking, the cells were lysed and click conjugation  
15 was used to attach the fluorescent molecule (KKL-2107) to the alkyne moiety of KKL-  
16 2098, facilitating purification and visualization of cross-linked molecules. Analysis of  
17 proteins using SDS-PAGE showed no fluorescent bands, indicating that KKL-2098 was  
18 not cross-linked to a protein (**Fig. S1**). However, analysis of RNA preparations from  
19 KKL-2098–treated cells revealed a fluorescent band that co-migrated with 23S rRNA on  
20 agarose gels (**Fig. 4a**). Similar results were obtained when cross-linking was repeated  
21 with RNA extracts from *M. tuberculosis* and *E. coli* (**Fig. S2**). Primer extension assays  
22 were used to confirm that KKL-2098 was cross-linked to 23S rRNA. Assays using RNA  
23 from KKL-2098–treated *M. smegmatis* cells reproducibly showed a prominent band that  
24 was not present in control reactions using RNA from cells treated with KKL-35 instead  
25 of KKL-2098 (KKL-35 will not cross-link but causes the same physiological response in  
26 the cells) (**Fig. 4b, Fig. S3**). This band indicated that reverse transcriptase activity was  
27 terminated after nucleotide 2505 (*E. coli* numbering), suggesting KKL-2098 was cross-  
28 linked to nucleotide  $\Psi$ 2504 (**Fig. 4b**). Primer extension on 23S rRNA from *E. coli* after  
29 cross-linking with KKL-2098 indicated modification of nucleotide C2452 (**Fig. S4**), which  
30 base pairs with  $\Psi$ 2504.<sup>22</sup>  $\Psi$ 2504 and C2452 are positioned at the base of H89, a  
31  
32  
33  
34  
35  
36  
37  
38  
39  
40  
41  
42  
43  
44  
45  
46  
47  
48  
49  
50  
51  
52  
53  
54  
55  
56  
57  
58  
59  
60



1  
2  
3 structure that extends from the PTC to the factor binding site (**Fig. 4c, d**).<sup>23</sup> Nucleotides  
4 that border the PTC and those located at the base of H89 adjacent to the PTC (**Fig. 5**)  
5 are highly conserved and essential for efficient ribosome function in bacteria.<sup>23,24</sup>  
6  
7  
8 Mutation of  $\Psi$ 2504, C2452 or other nearby nucleotides, as well as conformational  
9  
10 changes in H89, have been shown to have moderate to severe effects on translation  
11  
12 fidelity, ribosome function and/or cell growth.<sup>24-27</sup> Collectively, these data indicate that  
13  
14 the base of H89 is the target for KKL-35 and related 1,3,4-oxadiazole benzamides.  
15  
16  
17  
18  
19

### 20 21 **Docking and solvent mapping predict binding site for 1,3,4-oxadiazole** 22 23 **benzamides** 24

25  
26  
27 Guided by results from the cross-linking experiments, we performed *in silico* molecular  
28  
29 docking studies using the Autodock-Vina program.<sup>28</sup> KKL-35 was docked to a region of  
30  
31 the 50S ribosome encompassing the PTC and the full-length H89 to the edge of the  
32  
33 factor-binding site (**Fig. S5**). The 6 lowest energy structures had KKL-35 in the same  
34  
35 pocket at the base of H89 near nucleotides  $\Psi$ 2504 and C2452 (**Fig. 6**). The  
36  
37 conformation of KKL-35 within this pocket varied, but in all cases the main contributors  
38  
39 to the binding energy based on the docked conformation were the predicted polar  
40  
41 interactions between KKL-35 and H89 originating from the carbonyl oxygen atom and  
42  
43 the oxadiazole core (**Fig. 6**). The latter contribution is in agreement with experimental  
44  
45 evidence showing favorable electron donor capabilities for the 1,3,4-oxadiazole ring as  
46  
47 a result of a large dipole moment generated by the nitrogen atoms.<sup>29</sup> Docking  
48  
49 experiments using KKL-2098 and KKL-40 localized these compounds to the same  
50  
51 pocket, with similar docked conformations and binding energies as KKL-35 ( $\Delta G = -8.8$   
52  
53  
54  
55  
56  
57  
58  
59  
60

1  
2  
3 kcal/mol for KKL-35, -9.0 kcal/mol for KKL-2098, and -9.5 kcal/mol for KKL-40) (**Fig.**  
4  
5 **S5**). In some structures the oxadiazole-amide core was oriented in a conformation that  
6  
7 would place the azide group of KKL-2098 in position to cross-link with  $\Psi$ 2504 and  
8  
9 C2452, but in others the orientation of the oxadiazole-amide was reversed (**Fig. S5**).  
10  
11 The similar docked energies of the forward and reverse conformations are a result of  
12  
13 partial symmetry in the molecules based on the location H-donor and acceptor atoms in  
14  
15 the oxadiazole-amide core, and the phenyl-rings (**Fig. S5**). Therefore, the docking  
16  
17 studies predict a binding pocket for 1,3,4-oxadiazole benzamides at the base of H89,  
18  
19 but do not specify the conformation of the molecules within this pocket. Because the  
20  
21 ribosome structure bound by 1,3,4-oxadiazole benzamides may be subtly different from  
22  
23 the available crystal and cryo-EM structures, we cannot exclude the possibility that  
24  
25 these molecules bind in the PTC where they could contact the other face of the  $\Psi$ 2504-  
26  
27 C2452 base pair. Other antibiotics, including linezolid, bind in the PTC close to  $\Psi$ 2504  
28  
29 and C2452.<sup>30</sup> Unlike linezolid, KKL-35 and other oxadiazoles do not inhibit translation<sup>17</sup>,  
30  
31 so they would have to bind within the PTC in a manner that inhibited *trans*-translation  
32  
33 but not translation. Ongoing structural studies should provide more insight on the  
34  
35 binding site for 1,3,4-oxadiazole benzamides.  
36  
37  
38  
39  
40  
41  
42  
43  
44

45 We used a computational solvent mapping algorithm (FTMap) to assess solvent  
46  
47 accessibility and druggability of H89.<sup>31</sup> The FTMap server performs solvent mapping  
48  
49 using standard probes with variable chemical structures to identify probable drug  
50  
51 binding hot spots within a macromolecule.<sup>31</sup> These hot spots, typically located within  
52  
53 probe-cluster consensus sites (CS), are regions capable of binding a variety of  
54  
55 chemically diverse probes and are predicted to contribute significantly to the binding  
56  
57  
58  
59  
60

1  
2  
3 free energy.<sup>31,32</sup> Probe clustering was observed at several sites on H89 (**Fig. 6d**), but  
4  
5 the base region had one major hot spot which comprised four CSs (**Fig. 6d, Fig. S6**).  
6  
7 Structural alignment of docked KKL-35 with solvent mapping revealed that the predicted  
8  
9 binding pocket for KKL-35 superimposes with the solvent-mapped hot spot with probe  
10  
11 cluster coverage along the entire KKL-35 structure (**Fig. 6e**). These mapping data  
12  
13 together with the docking results for KKL-35 support the presence of a druggable  
14  
15 binding pocket for 1,3,4-oxadiazole benzamides at the base of H89 adjacent to the  
16  
17 PTC.  
18  
19  
20  
21  
22

### 23 **KKL-35 selectivity suggests structural changes in the ribosome during rescue**

24  
25  
26  
27 The data presented here indicate that KKL-35 bind to a highly conserved region of the  
28  
29 ribosome, and previous results showed that KKL-35 inhibits *trans*-translation but not  
30  
31 translation initiation, elongation, or termination.<sup>17</sup> Binding of a drug near the PTC might  
32  
33 be expected to interfere with translation and mutation of nucleotides that form the KKL-  
34  
35 35 binding site (for example U2460, U2492, U2493) (**Fig. 5b**), lead to significantly  
36  
37 decreased PTC activity and impaired cell growth.<sup>24-27</sup> However, KKL-35 did not inhibit  
38  
39 translation of mRNAs containing an in-frame stop codon when tested at concentrations  
40  
41 >100-fold above the IC<sub>50</sub> for inhibiting *trans*-translation *in vitro*.<sup>17</sup> KKL-2098 cross-linked  
42  
43 to 23S rRNA during *in vitro* translation of mRNAs containing an in-frame stop codon as  
44  
45 well as translation of nonstop mRNAs (**Fig. S2**), indicating that the binding site may be  
46  
47 accessible during normal translation. No cross-linking was observed in reactions that  
48  
49 did not contain mRNA (**Fig. S2**), suggesting that the inhibitors bind a structure that is  
50  
51 only present during translation. How could binding of KKL-35 to H89 inhibit *trans*-  
52  
53  
54  
55  
56  
57  
58  
59  
60

1  
2  
3 translation but not translation? One possible explanation is that binding of KKL-35 could  
4  
5 introduce polar interactions that limit flexibility of H89, preventing structural changes that  
6  
7 are required for ribosome rescue but not for translation. This selectivity might also  
8  
9 explain the ability KKL-35 to inhibit ribosome rescue by ArfA and ArfB in *E. coli* and *C.*  
10  
11 *croscensatus*: these alternative rescue pathways recognize nonstop translation complexes  
12  
13 in the absence of *trans*-translation.<sup>11,12</sup>  
14  
15  
16  
17  
18

19 In summary, the 1,3,4-oxadiazole benzamides present a unique chemical  
20  
21 scaffold that is distinct both in structure and mechanism of action from existing anti-  
22  
23 tuberculosis drugs.<sup>33,34</sup> KKL-35 and its analogs display promising bactericidal activity  
24  
25 against actively growing and non-replicating persister cells of MTB while exhibiting  
26  
27 minimal cytotoxicity against eukaryotic cells (Table 1).<sup>17</sup> Collectively, these properties  
28  
29 make the 1,3,4-oxadiazole benzamides good anti-tubercular drug candidates. In an  
30  
31 effort to circumvent current resistance trends, the druggable state of *trans*-translation in  
32  
33 MTB presents an excellent opportunity to develop novel anti-tuberculosis drugs.  
34  
35  
36  
37  
38

## 39 METHODS

40  
41  
42  
43 **Bacterial strains and growth conditions.** *M. tuberculosis* H37Rv,  $\Delta smpB::dif$ ,  
44  
45  $\Delta smpB::dif::smpB$  and  $\Delta ssrA::ssrA$  (gifts from Prof. Tanya Parish),<sup>16</sup> and the Erdman  
46  
47 TMC 107 (ATCC 35801) strain were cultured at 37 °C in 7H9 media (Difco, Becton  
48  
49 Dickinson, Franklin lakes, NJ) supplemented with 10% OADC (Middlebrook), 0.5%  
50  
51 glycerol, and 0.05% TWEEN 80. Solid medium plates were prepared using 7H10 agar  
52  
53  
54  
55  
56  
57  
58  
59  
60

1  
2  
3 (Difco) supplemented with 10% OADC (Middlebrook) and 0.5% glycerol. *E. coli*  $\Delta tolC$   
4  
5 (MG1655) was cultured in LB growth medium at 37 °C.  
6  
7

8  
9  
10 **MIC and MBC determination for KKL-35 against *M. tuberculosis*.** 1 ml culture was  
11 grown in 5 ml bottles to  $OD_{600} = 0.0125$  in 5 ml ink wells and KKL-35 was added at  
12 concentrations ranging from 0 to 1 mM. Cultures were incubated at 37 °C and the MIC  
13 was recorded as the minimum concentration of drug that inhibited visible growth. The  
14  
15  
16  
17  
18  
19  
20  
21  
22  
23  
24  
25  
26  
27  
28  
29  
30  
31  
32  
33  
34  
35  
36  
37  
38  
39  
40  
41  
42  
43  
44  
45  
46  
47  
48  
49  
50  
51  
52  
53  
54  
55  
56  
57  
58  
59  
60

**MIC and MBC determination for KKL-35 against *M. tuberculosis*.** 1 ml culture was grown in 5 ml bottles to  $OD_{600} = 0.0125$  in 5 ml ink wells and KKL-35 was added at concentrations ranging from 0 to 1 mM. Cultures were incubated at 37 °C and the MIC was recorded as the minimum concentration of drug that inhibited visible growth. The MBC was obtained through CFUs, which were determined by plating serial dilutions of cultures onto 7H10 agar plates. Plates were incubated for 3-4 weeks at 37 °C prior to enumeration of CFUs.

**Assessment of growth inhibition.** Auto-luminescent *M. tuberculosis* (LuxTB) was generated by transforming the wild-type Erdman strain with the pMlux plasmid, encoding the mycobacterial MOPS promoter driving expression of a synthetic GC-rich *luxCDABE* operon from *P. luminescens*.<sup>35,36</sup> LuxTB was cultured in 7H9 medium to  $OD_{600} = 0.0125$ . KKL-35 was added and the cultures were incubated at 37 °C. Luminescence readings were recorded every 24 h for 12 days using an Infinite M200 plate reader (Tecan Trading AG, Mannedorf, Switzerland).

***M. tuberculosis* SmpB depletion assays.** The *TetpsmpB::TetR* mutant was constructed by replacing 500 bp upstream of the *smpB* ATG start site with a tet operator (*tetO*)-containing mycobacterial promoter ( $P_{symbc}$ ).<sup>37</sup> This mutation was made by homologous recombination using a specialized mycobacterium phage system as previously described.<sup>38</sup> After the addition of the  $P_{symbc}$  promoter, the strain was transformed with a plasmid that integrates at the *attB* site and expresses the reverse

1  
2  
3 repressor TetR.<sup>37</sup> Repression of SmpB was achieved by incubation of cells with 300  
4  
5 ng/ml of anhydrotetracycline (Sigma-Aldrich, St. Louis, MO).  
6  
7

8  
9 ***M. tuberculosis* hypoxia assay.** For growth under hypoxia, MTB was grown in 17 ml  
10  
11 glass test tubes in triplicate and gradual hypoxia was generated using the Wayne  
12  
13 Model.<sup>19,39</sup> KKL-35 was added to hypoxic cultures at various concentrations and the  
14  
15 cultures incubated for 1 week. These cultures were then spread on 7H10 agar plates  
16  
17 and incubated at 37 °C for 3-4 weeks before enumeration of the CFUs.  
18  
19

20  
21  
22 **Genome sequencing.** Full genome sequencing of strain  $\Delta smpB::dif$  was performed by  
23  
24 generating a library from randomly sheared 350 bp genomic DNA fragments using a  
25  
26 TruSeq DNA Kit (Illumina Inc., San Diego, CA) following the manufacturer's protocol.  
27  
28 Paired-end sequencing was performed for 100 cycles using an Illumina HiSeq 2500 by  
29  
30 the University of Minnesota Genomics Center. Approximately 1.3 GB of data were  
31  
32 obtained representing >300 fold sequence coverage (NCBI BioProject accession  
33  
34 number PRJNA343132). High-quality paired-end reads were trimmed using Cutadapt  
35  
36 (<http://cutadapt.readthedocs.io/en/stable/guide.html#trimming-paired-end-reads>) and  
37  
38 mapped to the H37Rv reference genome sequence<sup>40</sup> using Geneious 6.0 (Biomatters  
39  
40 Ltd, Auckland, New Zealand). Sequence of the *smpB* region was independently verified  
41  
42 by sequencing of PCR amplicons covering open reading frames from *Rv3098c* -  
43  
44 *Rv3102c*.  
45  
46  
47  
48  
49

50  
51  
52 **qRT-PCR analysis of *smpB* expression.** Mid-exponential phase cultures of strains  
53  
54 H37Rv  $\Delta smpB::dif$ ,  $\Delta smpB::dif::smpB$  and  $\Delta ssrA::ssrA$  were harvested by centrifugation,  
55  
56 cell pellets were resuspended in buffer containing 10 mM Tris-HCl, 1 mM EDTA, 15  
57  
58  
59  
60

1  
2  
3 mg/ml lysozyme and incubated at 37°C for 16 h. RNA was extracted using the  
4  
5 E.Z.N.A.<sup>TM</sup> bacterial RNA kit (Omega Biotek, Norcross, GA). Residual DNA was  
6  
7 removed using the TURBO DNA-free<sup>TM</sup> kit (Life Technologies Corp., Grand Island, NY).  
8  
9 qRT-PCR was performed with the QuantiFast<sup>®</sup> SYBR<sup>®</sup> Green RT-PCR kit (Qiagen).  
10  
11 qRT-PCR reactions were prepared with 2X QuantiFast SYBR Green RT-PCR master  
12  
13 mix, 10 µM primers, 0.1 µl QuantiFast RT Mix, 1 ng RNA and were run on a  
14  
15 LightCycler<sup>®</sup> 480 with following cycle conditions: 50°C for 10 min, 95°C for 5 min, 35  
16  
17 cycles of 95°C for 10 s, 60°C for 10 s, and 72°C for 20 s with fluorescence quantification  
18  
19 for each cycle. A melting curve cycle of 95°C for 15 s, 60°C for 15 s, and 95°C with 2%  
20  
21 ramp rate was used to determine product specificity. A no reverse transcriptase qRT-  
22  
23 PCR control reaction was performed to test for contaminating DNA. Primers to express  
24  
25 the mature tmRNA were used for these studies.<sup>41</sup>  
26  
27  
28  
29  
30  
31  
32

33 tmRNA primer sequences: MSTSSRA-5 TGCAGGCAAGAGACCACCGTA, MTSSRA-6  
34  
35 CCGGTCACGCGAACTAGCCGAGA  
36  
37  
38

39 **Bioorthogonal photo-affinity labeling with KKL-2098.** Intracellular photo-labeling  
40  
41 was performed by adding either KKL-35 or KKL-2098 at the MIC to mid-exponential  
42  
43 cultures of *M. smegmatis*, *M. tuberculosis* or *E. coli*  $\Delta$ *tolC*. These cultures were grown  
44  
45 for 1 h and cells were harvested by centrifugation at 2716 g and resuspended in  
46  
47 phosphate buffered saline solution (1.2 g Na<sub>2</sub>HPO<sub>4</sub>, 0.22 g NaH<sub>2</sub>PO<sub>4</sub>, 8.5 g NaCl in 1L  
48  
49 pH 7.5). This suspension was irradiated with 312 nm UV light for 10 min and cells were  
50  
51 recovered by centrifugation. RNA extracts were prepared using the Norgen total RNA  
52  
53 preparation kit (Norgen Biotek Corp., Thorold, ON, Canada) according to the  
54  
55  
56  
57  
58  
59  
60

1  
2  
3 manufacturer's protocols and the purity of the isolated RNA assessed by agarose gel  
4  
5 electrophoresis.  
6  
7

8  
9 **Primer extension assays.** DNA oligonucleotides covering 23S rRNA were end-labeled  
10 with  $^{32}\text{P}$  using polynucleotide kinase (NEB, Ipswich, MA) according to the  
11 manufacturer's instructions. Primer extension assays<sup>42</sup> were performed using RNA from  
12 KKL-35 and KKL-2098-treated cells with Superscript II reverse transcriptase (Thermo  
13 Fisher Scientific, Bellefonte, PA) according to the manufacturer's instructions. The  
14 products were separated on an 8% polyacrylamide urea gel and visualized using a  
15 Typhoon 9410 imager (GE Healthcare, Tyrone, PA). These experiments were repeated  
16 using Superscript IV and Sunscript reverse transcriptase for confirmation of modified  
17 sites.  
18  
19  
20  
21  
22  
23  
24  
25  
26  
27  
28  
29

30  
31  
32 Oligonucleotide sequences used in the primers extension assays:  
33  
34  
35

36 **M. smegmatis 23S rRNA primers**  
37

38  
39 MS1 - TGTTGTAAGTTTTCGGCCGG  
40

41  
42 MS2 - CACGACGTTCTAAACCCAGC  
43

44  
45 MS3 - GCGCGTAACGAGCATCTTTA  
46

47  
48 MS4 - ACCTGTGTTGGTTTGGGGTA  
49

50  
51 MS5 - ATCAACCCGTTGTCCATCGA  
52

53  
54 MS6 - ACACGCTTAGGGGCCTTAG  
55  
56  
57  
58  
59  
60



1  
2  
3 MS7 - ACACACCACTACACCACACA  
4

5  
6 MS8 - GCCATTTCCGCTAACCACAA  
7  
8

9  
10 **E. coli 23S rRNA primers**  
11

12  
13 EC 1 - GGACACGTGGTATCCTGTCTG  
14

15  
16 EC 2 - AACTGGGCGTTAAGTTGCAG  
17  
18

19  
20 EC 3 - GGTCATCCCGACTTACCAA  
21

22  
23 EC 4 - GATGGGAAACAGGTTAATATTCCT  
24

25  
26 EC 5 - TGATCGAAGCCCCGGTAA  
27  
28

29  
30 EC 6 - AGGTCATAGTGATCCGGTGG  
31

32  
33 EC 7 - TACGCGAGCTGGGTTTAGAA  
34

35  
36 EC 8 - GTACTAATGAACCGTGAGGCTTAA  
37  
38

39  
40 **The copper catalyzed azide-alkyne Huisgen cycloaddition (AAHC) click**  
41  
42 **conjugation assay**  
43  
44

45 **RNA:** click conjugation reactions were performed in a 20  $\mu$ l scale by combining 8  $\mu$ l  
46 acetonitrile (final 40 % v/v), KKL-2107 (1 mM final), 2  $\mu$ l 1M Hepes pH 7.4 (final 100  
47  $\mu$ M), 8.6  $\mu$ l RNA solution, 2  $\mu$ l premixed solution of CuSO<sub>4</sub>/THPTA (final concentrations  
48 0.1 mM and 1 mM respectively) and NH<sub>2</sub>NH<sub>2</sub> (final concentration of 0.1 mM). Samples  
49  
50  
51  
52  
53  
54  
55  
56 were mixed and the reaction was incubated at room temperature for 15 min. 15  $\mu$ l 2X  
57  
58  
59  
60

1  
2  
3 formamide loading buffer was added and the sample was incubated at 65 °C for 10 min.

4  
5 Samples were analyzed by gel electrophoresis on a 1% agarose TAE gel.  
6  
7

8  
9  
10 **Protein:** KKL-35 or KKL-2098-treated cell pellets were resuspended in lysis buffer (100  
11 mM NaH<sub>2</sub>PO<sub>4</sub> (pH 7.5), 100 mM NaCl, 0.1% SDS, 2 mM BME), lysed by sonication, and  
12 clarified by centrifugation at 22,000 *g* for 10 min. The lysate was then subjected to click  
13 conjugation by mixing 100 μl acetonitrile, KKL-2107 (final concentration 1 mM), 172 μl  
14 clarified lysate, a pre-mixed solution of CuSO<sub>4</sub>/THPTA (final concentrations 0.4 mM and  
15 2 mM respectively) and NH<sub>2</sub>NH<sub>2</sub> (final concentration of 0.1 mM). Reactions were  
16 incubated at room temperature for 3 h with gentle agitation and protein was precipitated  
17 by addition of acetone. The recovered protein pellet was air-dried and re-dissolved in  
18 binding buffer (100 mM Na<sub>3</sub>PO<sub>4</sub>, 100 mM NaCl, 0.1% SDS, 2 mM BME). For affinity  
19 chromatography, NeutrAvidin (Thermo Fisher Scientific, Bellefonte, PA) agarose resin  
20 was equilibrated in binding buffer according to the manufacturer's protocols. A mixture  
21 of the resin and lysate was incubated for 1 h at room temperature with gentle agitation  
22 then transferred to a column. The column was washed with 10 volumes of binding  
23 buffer, the resin was transferred to a clean tube, and protein was eluted by addition of  
24 1X SDS sample buffer (34.2 mM Tris pH 6.8, 13.1 mM glycerol (w/v), 1% SDS, 0.01%  
25 bromophenol blue) and incubation at 95 °C for ~ 5 min. Samples were analyzed by SDS  
26 PAGE.  
27  
28  
29  
30  
31  
32  
33  
34  
35  
36  
37  
38  
39  
40  
41  
42  
43  
44  
45  
46  
47  
48

49  
50  
51 ***In vitro* photo-labeling and click conjugation.** Assays were set up using the  
52 PURExpress *in vitro* protein synthesis kit (NEB, Ipswich, MA) according to the  
53 manufacturer's protocols. The reactions were performed with: no DNA template, a  
54  
55  
56  
57  
58  
59  
60

1  
2  
3 nonstop DHFR template, the full length DHFR gene, full length DHFR gene with 0  
4 bases after the stop codon or full length DHFR gene with 33 bases after the stop codon.  
5  
6  
7  
8 <sup>16, 43</sup> KKL-2098 (final concentration 1  $\mu$ M) was added to a mixture of assay components  
9  
10 and the samples were incubated at room temperature for 1 h. Samples were placed on  
11  
12 ice, irradiated with 312 nm UV light for 10 min, and used to set up click conjugation  
13  
14 assays in the presence of KKL-2107 (final concentration 0.5 mM). After incubating for  
15  
16 30 min, an equal volume of 2X formamide loading buffer was added and the tubes were  
17  
18 incubated at 65 °C for 10 min. The samples were resolved on a 1% agarose gel. The  
19  
20 gel was first scanned for fluorescence (to visualize the conjugated probe) then stained  
21  
22 with ethidium bromide to visualize the RNA.  
23  
24  
25  
26  
27

28 ***In silico* molecular docking and solvent mapping.** Molecular docking studies were  
29  
30 performed with the AutoDock Vina program<sup>28</sup> utilizing the AutoDock tools graphical  
31  
32 interface. Energy minimizations for KKL-35 and KKL-2098 were performed using the  
33  
34 Open Babel module. Modeling, structural manipulation and visualization were  
35  
36 performed using PyMOL (Schrödinger). Receptor grid maps were generated using the  
37  
38 AutoGrid module and KKL-35 or KKL-2098 docked using the Lamarckian genetic  
39  
40 algorithm. Docking for KKL-35 and KKL-2098 to the 70S ribosome was guided by  
41  
42 results from the cross-linking experiments with KKL-2098. The dimensions of the dock-  
43  
44 search space were adjusted to encompass the peptidyl-transfer center and helix 89 of  
45  
46 the 50S ribosomal crystal structure. These studies were performed with multiple crystal  
47  
48 structures: PDB ID: 4ABR, 4V69, 3DLL, 4V7T. The best binding conformations were  
49  
50 selected from the 10 generated from the docking event based on a criterion combining  
51  
52 the highest dock score and the lowest root mean square deviation values (RMSD < 1).  
53  
54  
55  
56  
57  
58  
59  
60

1  
2  
3 **Computational solvent mapping.** The H89 structure was extracted from the protein  
4  
5  
6  
7  
8  
9  
10  
11  
12  
13  
14  
15  
16  
17  
18  
19  
20  
21  
22  
23  
24  
25  
26  
27  
28  
29  
30  
31  
32  
33  
34  
35  
36  
37  
38  
39  
40  
41  
42  
43  
44  
45  
46  
47  
48  
49  
50  
51  
52  
53  
54  
55  
56  
57  
58  
59  
60

**Computational solvent mapping.** The H89 structure was extracted from the protein databank ribosome structure (PDB ID: 4ABR). All water molecules and ions were removed and mapping performed using the FTMap algorithm<sup>31,32</sup> (Boston University, MA) remotely through its servers online (<http://ftmap.bu.edu>). The entire surface of H89 was scanned with a mini probe library of 16 organic small molecules with variable hydrophobic and hydrogen bonding properties. The program utilized CHARMM energy minimized conformations for all the probes to scope from potential binding sites on H89. The algorithm retained six bound clusters with the lowest mean interaction energies for each probe. Probe-cluster consensus sites (CS) were then identified from congregated groups of structurally diverse probe. Each of the CSs represented a potential binding hot spot within H89 and was ranked based on the number of probe clusters it contained. The CS with the largest number of probe clusters characterized the most probable small molecule binding sites.

## ASSOCIATED CONTENT

### Supporting information

The supporting information file is available free of charge on the ACS publications website.

Results for additional *in vitro* biochemical assays, *in silico* molecular modeling and experimental details for the chemical synthesis (PDF)

### Accession numbers

1  
2  
3 Whole genome sequencing results for the MTB SmpB deletion strains are accessible  
4  
5 via GenBank using the accession numbers SAMN05907893 and SAMN05907849.  
6  
7  
8  
9

## 10 **AUTHOR INFORMATION:**

### 11 **Author Contributions**

12  
13  
14 J.N.A., K.C.K. and J.S.C. conceived the study. J.N.A., K.C.K, A.D.B. and J.S.C.  
15  
16 designed the experiments. J.N.A performed chemical synthesis and compound  
17  
18 characterization, *in vitro* biochemical analysis, target identification and *in silico* modeling  
19  
20 studies. J.N.A and K.C.K performed the primer extension assays. P.S.M. and T.L.  
21  
22 screened for activity against MTB, performed *smpB* knock-out experiments and carried  
23  
24 out the MTB hypoxia model assays. N.D.P. and A.D.B. generated, analyzed and  
25  
26 interpreted full genome sequencing data and qRT-PCR data for MTB strains H37Rv,  
27  
28  $\Delta smpB::dif$ ,  $\Delta smpB::dif::smpB$ , and  $\Delta ssrA::ssrA$ . J.N.A., K.C.K., J.S.C. and A.D.B.  
29  
30 prepared and wrote the manuscript.  
31  
32  
33  
34  
35  
36

### 37 **Current address**

38  
39 Paulo S. Manzanillo: Genentech Immunology Department, San Francisco, California  
40  
41 USA; Nicholas D. Peterson: University of Massachusetts Medical School, Worcester,  
42  
43 Massachusetts USA; Tricia Lundrigan: Department of Cellular and Molecular  
44  
45 Pharmacology, University of California, San Francisco, California USA.  
46  
47  
48

### 49 **Notes**

50  
51 The authors declare no competing financial interest.  
52  
53  
54  
55  
56

## 57 **ACKNOWLEDGEMENTS**

1  
2  
3 The authors thank Yusuke Minato for assistance with MTB MIC determinations, Teresa  
4 Repasy for assistance with MTB studies, Tanya Parish for providing strains, and Amber  
5 Miller for performing toxicity screens against HeLa cells. J.N.A. is grateful to Steven J.  
6 Benkovic for use of chemical synthesis facilities. This work was supported by NIH  
7 grants GM068720 and AI132275 to K.C.K., DP1AI124619 to J.S.C., and NIH grant  
8 AI123146 and the Bill and Melinda Gates Foundation Grand Challenges Explorations  
9 grant to A.D.B.  
10  
11  
12  
13  
14  
15  
16  
17  
18  
19  
20  
21  
22  
23  
24  
25  
26  
27

## 28 REFERENCES

- 29  
30  
31  
32  
33 1. World Health Organization. (2015) Global tuberculosis report. World Health  
34 Organization Geneva, Switzerland.  
35 [http://www.who.int/tb/publications/global\\_report/en/](http://www.who.int/tb/publications/global_report/en/).  
36  
37  
38  
39 2. Kurz, S. G., Furin, J. J., and Bark, C. M. (2016) Drug-Resistant Tuberculosis:  
40 Challenges and Progress. *Infect. Dis. Clin. North Am.* 30, 509-522. DOI:  
41 10.1016/j.idc.2016.02.010  
42  
43  
44  
45  
46 3. Keiler, K. C., and Alumasa, J. N. (2013) The potential of *trans*-translation  
47 inhibitors as antibiotics. *Future Microbiol.* 8, 1235-1237. DOI:  
48 10.2217/fmb.13.110.  
49  
50  
51  
52  
53 4. Keiler, K. C. (2008) Biology of *trans*-translation. *Annu. Rev. Microbiol.* 62, 133-  
54 151. DOI: 10.1146/annurev.micro.62.081307.162948.  
55  
56  
57  
58  
59  
60

- 1  
2  
3 5. Keiler, K. C., Waller, P. R., and Sauer, R. T. (1996) Role of a peptide tagging  
4 system in degradation of proteins synthesized from damaged messenger RNA.  
5  
6 *Science*. 271, 990-993.  
7  
8
- 9  
10 6. Giudice, E., Macé, K., and Gillet, R. (2014) *Trans*-translation exposed:  
11 understanding the structures and functions of tmRNA-SmpB. *Front. Microbiol.* 5,  
12 113. DOI: 10.3389/fmicb.2014.00113.  
13  
14
- 15 7. Himeno, H., Kurita, D., and Muto, A. (2014) tmRNA-mediated *trans*-translation as  
16 the major ribosome rescue system in a bacterial cell. *Front. Genet.* 5, 66. DOI:  
17 10.3389/fgene.2014.00066.  
18  
19
- 20 8. Himeno, H., Nameki, N., Kurita, D., Muto, A., and Abo, T. (2015) Ribosome  
21 rescue systems in bacteria. *Biochimie.* 114, 102-112. DOI:  
22 10.1016/j.biochi.2014.11.014.  
23  
24
- 25 9. Ito, K., Chadani, Y., Nakamori, K., Chiba, S., Akiyama, Y., and Abo, T. (2011)  
26 Nascentome analysis uncovers futile protein synthesis in *Escherichia coli*. *PLoS*  
27 *One.* 6, e28413. DOI: 10.1371/journal.pone.0028413.  
28  
29
- 30 10. Keiler, K. C. 2015. Mechanisms of ribosome rescue in bacteria. *Nat. Rev.*  
31 *Microbiol.* 13, 285-297. DOI: 10.1038/nrmicro3438.  
32  
33
- 34 11. Chadani, Y., Ono, K., Kutsukake, K., and Abo, T. (2011) *Escherichia coli* YaeJ  
35 protein mediates a novel ribosome-rescue pathway distinct from *ssrA* and *ArfA*-  
36 mediated pathways. *Mol. Microbiol.* 80, 772-785. DOI: 10.1111/j.1365-  
37 2958.2011.07607.x.  
38  
39  
40  
41  
42  
43  
44  
45  
46  
47  
48  
49  
50  
51  
52  
53  
54  
55  
56  
57  
58  
59  
60

- 1  
2  
3  
4  
5  
6  
7  
8  
9  
10  
11  
12  
13  
14  
15  
16  
17  
18  
19  
20  
21  
22  
23  
24  
25  
26  
27  
28  
29  
30  
31  
32  
33  
34  
35  
36  
37  
38  
39  
40  
41  
42  
43  
44  
45  
46  
47  
48  
49  
50  
51  
52  
53  
54  
55  
56  
57  
58  
59  
60
12. Chadani, Y., Ito, K., Kutsukake, K., and Abo, T. (2012) ArfA recruits release factor 2 to rescue stalled ribosomes by peptidyl-tRNA hydrolysis in *Escherichia coli*. *Mol. Microbiol.* *86*, 37-50. DOI: 10.1111/j.1365-2958.2012.08190.x.
13. Shi, W., Zhang, X., Jiang, X., Yuan, H., Lee, J. S, Barry, C. E., Wang, H., Zhang, W., and Zhang, Y. (2011) Pyrazinamide inhibits *trans*-translation in *Mycobacterium tuberculosis*. *Science*. *333*, 1630-2. DOI: 10.1126/science.1208813.
14. Dillon, N. A., Peterson, N. D., Feaga, H. A., Keiler, K. C., and Baughn, A. D. (2017) Anti-tubercular activity of pyrazinamide is independent of *trans*-Translation and RpsA. *Sci. Rep.* (In press)
15. Zhang, Y. J., Ioerger, T. R., Huttenhower, C., Long, J. E., Sasseti, C. M., Sacchettini, J. C., and Rubin, E. J. (2012) Global assessment of genomic regions required for growth in *Mycobacterium tuberculosis*. *PLoS Pathog.* *8*, e1002946. DOI: 10.1371/journal.ppat.1002946.
16. Personne, Y., and Parish, T. (2014) *Mycobacterium tuberculosis* possesses an unusual tmRNA rescue system. *Tuberculosis*. *94*, 34-42. DOI: 10.1016/j.tube.2013.09.007.
17. Ramadoss, N. S., Alumasa, J. N., Cheng, L., Wang, Y., Li, S., Chambers, B. S., Chang, H., Chatterjee, A. K., Brinker, A., Engels, I. H., and Keiler, K. C. (2013) Small molecule inhibitors of *trans*-translation have broad-spectrum antibiotic activity. *Proc. Natl. Acad. Sci. USA*. *110*, 10282-10287. DOI: 10.1073/pnas.1302816110.



- 1  
2  
3  
4  
5  
6  
7  
8  
9  
10  
11  
12  
13  
14  
15  
16  
17  
18  
19  
20  
21  
22  
23  
24  
25  
26  
27  
28  
29  
30  
31  
32  
33  
34  
35  
36  
37  
38  
39  
40  
41  
42  
43  
44  
45  
46  
47  
48  
49  
50  
51  
52  
53  
54  
55  
56  
57  
58  
59  
60
18. Goralski, T. D., Dewan, K. K., Alumasa, J. N., Avanzato, V., Place, D. E., Markley, R. L., Katkere, B., Rabadi, S. M., Bakshi, C. S., Keiler, K. C., and Kirimanjeswara, G. S. (2016) Inhibitors of Ribosome Rescue Arrest Growth of *Francisella tularensis* at All Stages of Intracellular Replication. *Antimicrob. Agents Chemother.* *60*, 3276-3282. DOI: 10.1128/AAC.03089-15.
19. Sohaskey, C. D., and Voskuil, M. I. (2015) *In vitro* models that utilize hypoxia to induce non-replicating persistence in Mycobacteria. *Methods Mol. Biol.* *1285*, 201-213. DOI: 10.1007/978-1-4939-2450-9\_11.
20. Sumranjit, J., and Chung, S. J. (2013) Recent Advances in Target Characterization and Identification by Photoaffinity Probes. *Molecules.* *18*, 10425-10451. DOI: 10.3390/molecules180910425.
21. Alumasa, J. N., and Keiler, K. C. (2015) Clicking on *trans*-translation drug targets. *Front. Microbiol.* *6*, 498. DOI: 10.3389/fmicb.2015.00498.
22. Eyal, Z., Matzov, D., Krupkin, M., Paukner, S., Riedl, R., Rozenberg, H., Zimmerman, E., Bashan, A., and Yonath, A. (2016) A novel pleuromutilin antibacterial compound, its binding mode and selectivity mechanism. *Sci Rep.* *6*:39004. DOI: 10.1038/srep39004.
23. Polacek, N., and Mankin, A. S. (2005) The ribosomal peptidyl transferase center: structure, function, evolution, inhibition. *Crit. Rev. Biochem. Mol. Biol.* *40*, 285-311. DOI: 10.1080/10409230500326334.
24. Burakovsky, D. E., Sergiev, P. V., Steblyanko, M. A., Konevega, A. L., Bogdanov, A. A., and Dontsova, O. A. (2011) The structure of helix 89 of 23S rRNA is

- 1  
2  
3 important for peptidyl transferase function of *Escherichia coli* ribosome. *FEBS*  
4  
5 *Lett.* *585*, 3073-3078. DOI: 10.1016/j.febslet.2011.08.030.  
6  
7
- 8 25. Porse, B. T., and Garrett, R. A. (1995) Mapping important nucleotides in the  
9  
10 peptidyl transferase centre of 23S rRNA using a random mutagenesis approach.  
11  
12 *J. Mol. Biol.* *249*, 1-10. DOI: 10.1006/jmbi.1995.0276.  
13  
14
- 15 26. O'Connor, M., and Dahlberg, A. E. (1995) The involvement of two distinct regions  
16  
17 of 23S ribosomal RNA in tRNA selection. *J. Mol. Biol.* *254*, 838-847. DOI:  
18  
19 10.1006/jmbi.1995.0659.  
20  
21
- 22 27. Long, K. S., Poehlsgaard, J., Hansen, L. H., Hobbie, S. N., Böttger, E. C., Vester,  
23  
24 B. (2009) Single 23S rRNA mutations at the ribosomal peptidyl transferase  
25  
26 centre confer resistance to valnemulin and other antibiotics in *Mycobacterium*  
27  
28 *smegmatis* by perturbation of the drug binding pocket. *Mol. Microbiol.* *71*, 1218-  
29  
30 1227. DOI: 10.1111/j.1365-2958.2009.06596.x.  
31  
32  
33
- 34 28. Trott, O., and Olson, A. J. (2010) AutoDock Vina: improving the speed and  
35  
36 accuracy of docking with a new scoring function, efficient optimization and  
37  
38 multithreading. *J. Comput. Chem.* *31*, 455-461. DOI: 10.1002/jcc.21334.  
39  
40
- 41 29. Boström, J., Hogner, A., Llinàs, A., Wellner, E., and Plowright, A. T. (2012)  
42  
43 Oxadiazoles in medicinal chemistry. *J. Med. Chem.* *55*, 1817-1830. DOI:  
44  
45 10.1021/jm2013248.  
46  
47
- 48 30. Belousoff, M. J., Eyal, Z., Radjainia, M., Ahmed, T., Bamert, R. S., Matzov, D.,  
49  
50 Bashan, A., Zimmerman, E., Mishra, S., Cameron, D., Elmlund, H., Peleg, A. Y.,  
51  
52 Bhushan, S., Lithgow, T., and Yonath, A. (2017) Structural Basis for Linezolid  
53  
54  
55  
56  
57  
58  
59  
60

- 1  
2  
3 Binding Site Rearrangement in the *Staphylococcus aureus* Ribosome. *MBio.* 8,  
4  
5 pii: e00395-17. doi: 10.1128/mBio.00395-17.  
6  
7
- 8 31. Kozakov, D., Grove, L. E., Hall, D. R., Bohnuud, T., Mottarella, S. E., Luo, L., Xia,  
9  
10 B., Beglov, D., and Vajda, S. (2015) The FTMap family of web servers for  
11  
12 determining and characterizing ligand-binding hot spots of proteins. *Nat. Protoc.*  
13  
14 10, 733-755. DOI: 10.1038/nprot.2015.043.  
15  
16
- 17 32. Kozakov, D., Hall, D. R., Chuang, G. Y., Cencic, R., Brenke, R., Grove, L. E.,  
18  
19 Beglov, D., Pelletier, J., Whitty, A., and Vajda, S. (2011) Structural conservation  
20  
21 of druggable hot spots in protein–protein interfaces. *Proc. Natl Acad. Sci. USA.*  
22  
23 108, 13528-13533. DOI: 10.1073/pnas.1101835108.  
24  
25
- 26 33. Hoagland, D. T, Liu, J., Lee, R. B., Lee, and R. E. (2016) New agents for the  
27  
28 treatment of drug-resistant *Mycobacterium tuberculosis*. *Adv. Drug Deliv. Rev.*  
29  
30 102, 55-72. DOI: 10.1016/j.addr.2016.04.026.  
31  
32
- 33 34. Silva, J. P., Appelberg, R., and Gama, F. M. (2016) Antimicrobial peptides as  
34  
35 novel anti-tuberculosis therapeutics. *Biotechnol. Adv.* 34, 924-940. DOI:  
36  
37 10.1016/j.biotechadv.2016.05.007.  
38  
39
- 40 35. Pledger, G. W., Laxer, K. D., Sahlroot, J. T., Taylor, M. R., Cereghino, J. J.,  
41  
42 McCormick, C., Whitley, L., and Manning, L. W. (1992) Pharmacokinetic and  
43  
44 dose tolerability study of ADD 94057 in comedicated patients with partial  
45  
46 seizures. *Epilepsia.* 33, 112-118.  
47  
48
- 49 36. Eisele, N. A., Ruby, T., Jacobson, A., Manzanillo, P. S., Cox, J. S., Lam, L.,  
50  
51 Mukundan, L., Chawla, A., and Monack, D. M. (2013) Salmonella require the fatty  
52  
53 acid regulator PPAR $\delta$  for the establishment of a metabolic environment essential  
54  
55  
56  
57  
58  
59  
60

1  
2  
3 for long-term persistence. *Cell Host Microbe*. 14, 171-182. DOI:

4  
5  
6 10.1016/j.chom.2013.07.010.

7  
8 37. Klotzsche, M., Ehrt, S., and Schnappinger, D. (2009) Improved tetracycline  
9  
10 repressors for gene silencing in mycobacteria. *Nucleic Acids Res*. 37, 1778-  
11  
12 1788. DOI: 10.1093/nar/gkp015.

13  
14  
15 38. Glickman, M. S., Cox, J. S., and Jacobs, W. R. Jr. (2000) A novel mycolic acid  
16  
17 cyclopropane synthetase is required for cording, persistence, and virulence of  
18  
19 *Mycobacterium tuberculosis*. *Mol. Cell*. 5, 717-727.

20  
21  
22 39. Wayne, L. G., and Hayes, L. G. (1996) An *in vitro* model for sequential study of  
23  
24 shiftdown of *Mycobacterium tuberculosis* through two stages of nonreplicating  
25  
26 persistence. *Infect. Immun*. 64, 2062–2069.

27  
28  
29 40. Cole, S. T., Brosch, R., Parkhill, J., Garnier, T., Churcher, C., Harris, D., Gordon,  
30  
31 S. V., Eiglmeier, K., Gas, S., Barry, C. E., Tekaiia, F., Badcock, K., Basham, D.,  
32  
33 Brown, D., Chillingworth, T., Connor, R., Davies, R., Devlin, K., Feltwell, T.,  
34  
35 Gentles, S., Hamlin, N., Holroyd, S., Hornsby, T., Jagels, K., Krogh, A., McLean,  
36  
37 J., Moule, S., Murphy, L., Oliver, K., Osborne, J., Quail, M. A., Rajandream, M. A.,  
38  
39 Rogers, J., Rutter, S., Seeger, K., Skelton, J., Squares, R., Squares, S., Sulston,  
40  
41 J. E., Taylo, K., Whitehead, S., and Barrell, B. G. (1998) Deciphering the biology  
42  
43 of *Mycobacterium tuberculosis* from the complete genome sequence. *Nature*.  
44  
45 393, 537-544.

46  
47  
48 41. Andini, N., and Nash, K. A. (2011) Expression of tmRNA in mycobacteria is  
49  
50 increased by antimicrobial agents that target the ribosome. *FEMS Microbiol. Lett*.  
51  
52 322, 172–179. DOI: 10.1111/j.1574-6968.2011.02350.x.

- 1  
2  
3 42. Mortorin, Y., Muller, S., Behm-Ansmant, I., and Branlant, C. (2007) Identification  
4  
5 of Modified Residues in RNAs by Reverse Transcription-Based Methods.  
6  
7 *Methods Enzymol.* 425, 21-53. DOI: 10.1016/S0076-6879(07)25002-5.  
8  
9  
10 43. Feaga, H. A., Quickel, M. D., Hankey-Giblin, P. A., and Keiler, K. C. (2016)  
11  
12 Human Cells Require Non-stop Ribosome Rescue Activity in Mitochondria.  
13  
14 *PLoS Genet.* 12, e1005964. DOI: 10.1371/journal.pgen.1005964.  
15  
16  
17  
18  
19  
20  
21  
22  
23  
24  
25  
26  
27  
28  
29  
30  
31  
32  
33  
34  
35  
36  
37  
38  
39  
40  
41  
42  
43  
44  
45  
46  
47  
48  
49  
50  
51  
52  
53  
54  
55  
56  
57  
58  
59  
60

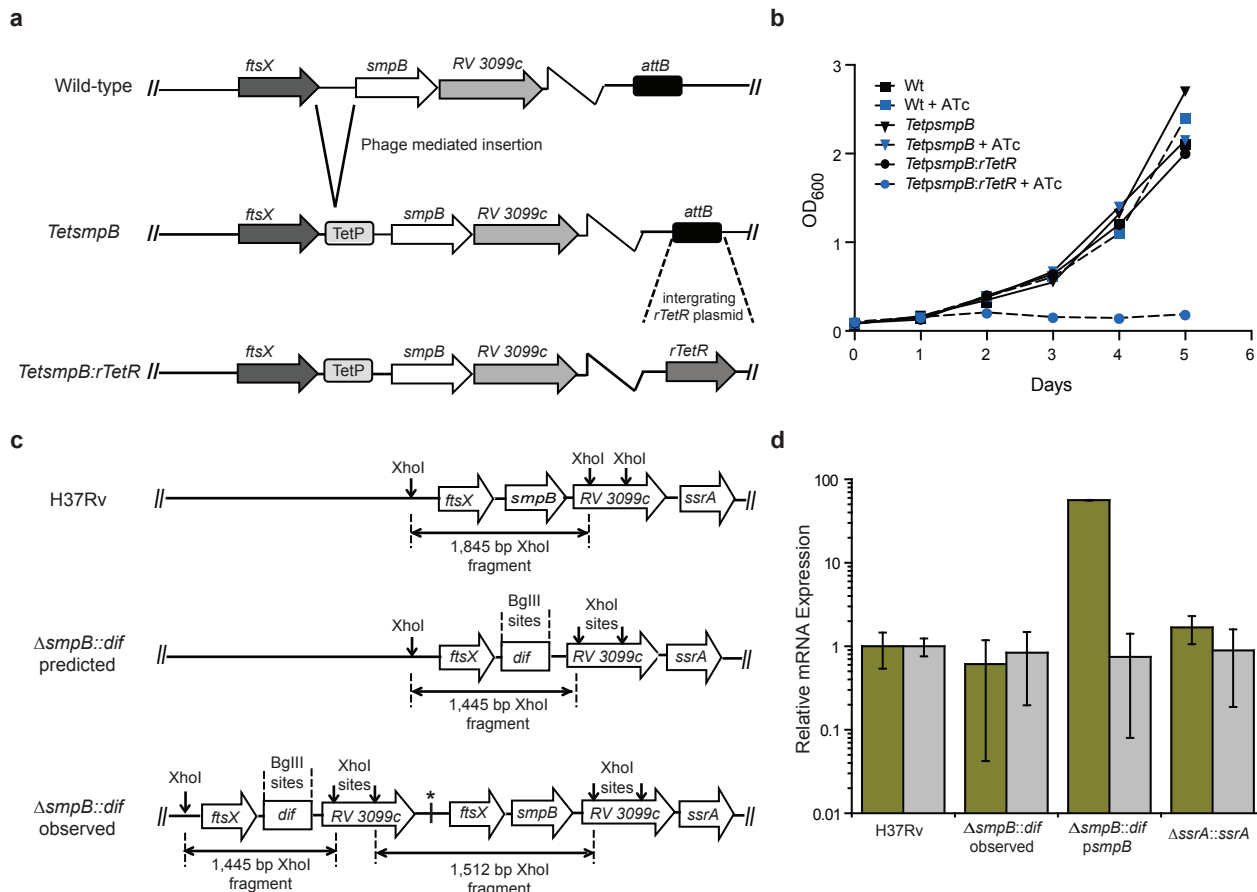


**Figure 1. SmpB is essential in MTB.** (a) Schematic illustration for the design of the *smpB* depletion constructs in MTB. (b) Growth curves for the SmpB depletion and control strains. (c) Schematic diagram of the *smpB* locus in the parental H37Rv strain, the reported  $\Delta smpB::dif^{A6}$  and  $\Delta smpB::dif$  observed from whole genome sequencing showing that the  $\Delta smpB::dif$  strain has a copy of *smpB*. (d) qRT-PCR analysis showing that both *ssrA* and *smpB* are expressed in the  $\Delta smpB::dif$  strain. *smpB* (yellow) and *ssrA* (gray) mRNA levels in mid-exponential phase MTB cells were quantified by qRT-PCR and normalized to the housekeeping gene *sigA*. Mean values from 3 technical replicates of one biological sample are shown with error bars indicating the standard deviation.

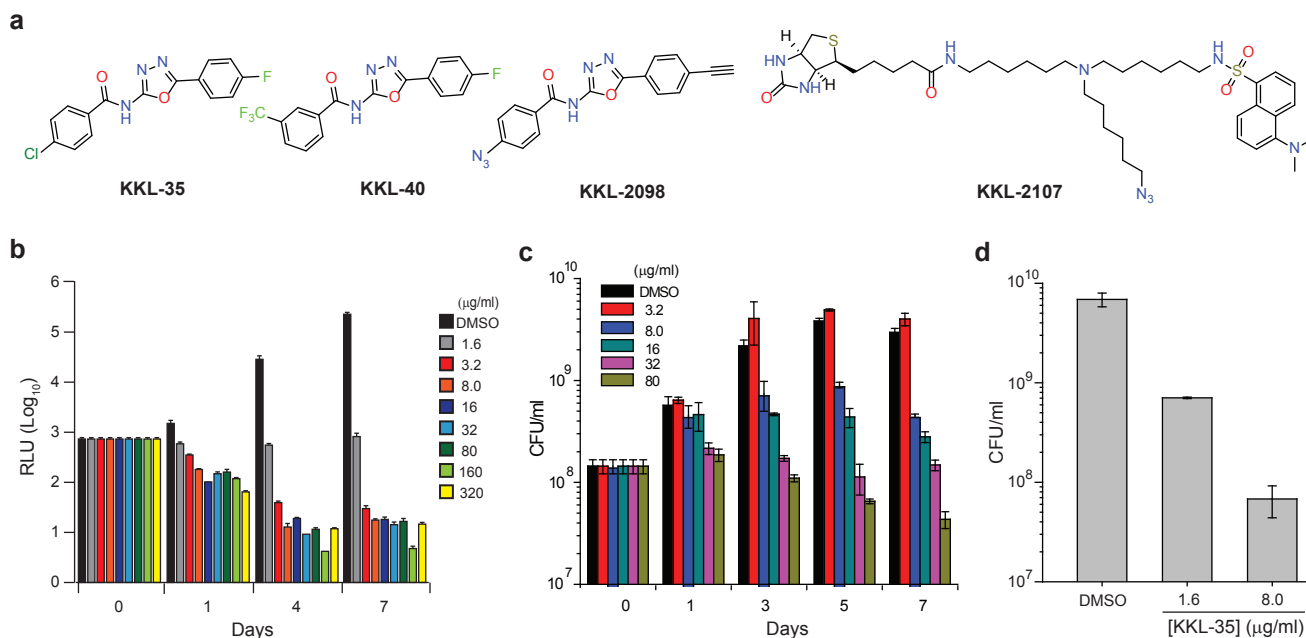


**Figure 2. Compound structures and activity for KKL-35 against MTB.** (a) Structures of the 1,3,4-oxadiazole benzamides KKL-35, KKL-40, the photo-labile click probe KKL-2098 and the tri-functional fluorescent molecule, KKL-2107. (b) Growth inhibitory profiles for MTB cultures treated with KKL-35 and monitored by luminescence. (c) CFU counts for MTB liquid cultures treated with KKL-35. (d) CFUs recovered from MTB cells grown using the hypoxia model for non-replicating persisters treated with KKL-35. The median from two replicates is shown with error bars indicating the standard deviation.

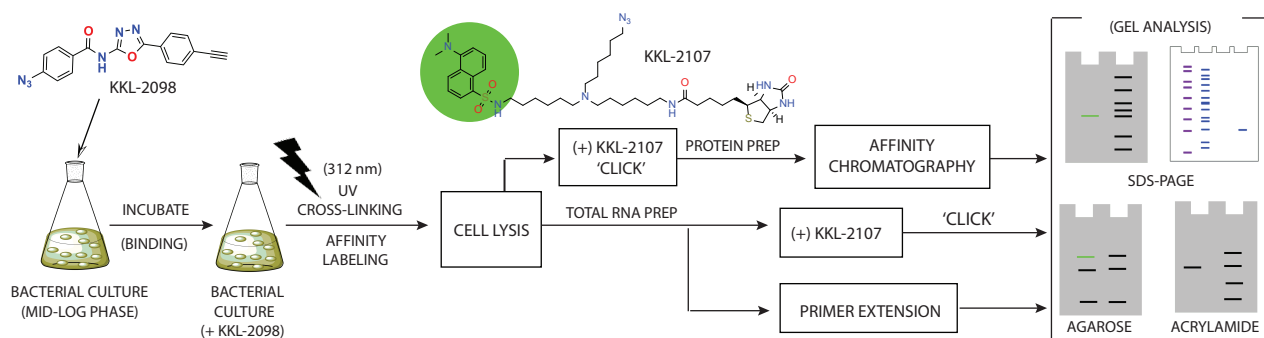


**Figure 3. Target identification work-flow.** The photo-labile probe KKL-2098 was added to a growing bacterial culture. Cells were irradiated with UV light to activate the probe and enable cross-linking. Cells were lysed and protein was denatured and subjected to click chemistry with the fluorescent affinity compound KKL-2107, and analyzed by SDS-PAGE. Alternatively, total RNA was purified and used in click conjugation assays with KKL-2107 or primer extension assays to detect RNA modification. Agarose or polyacrylamide gel electrophoresis was used to visualize and identify the probe-linked macromolecule.



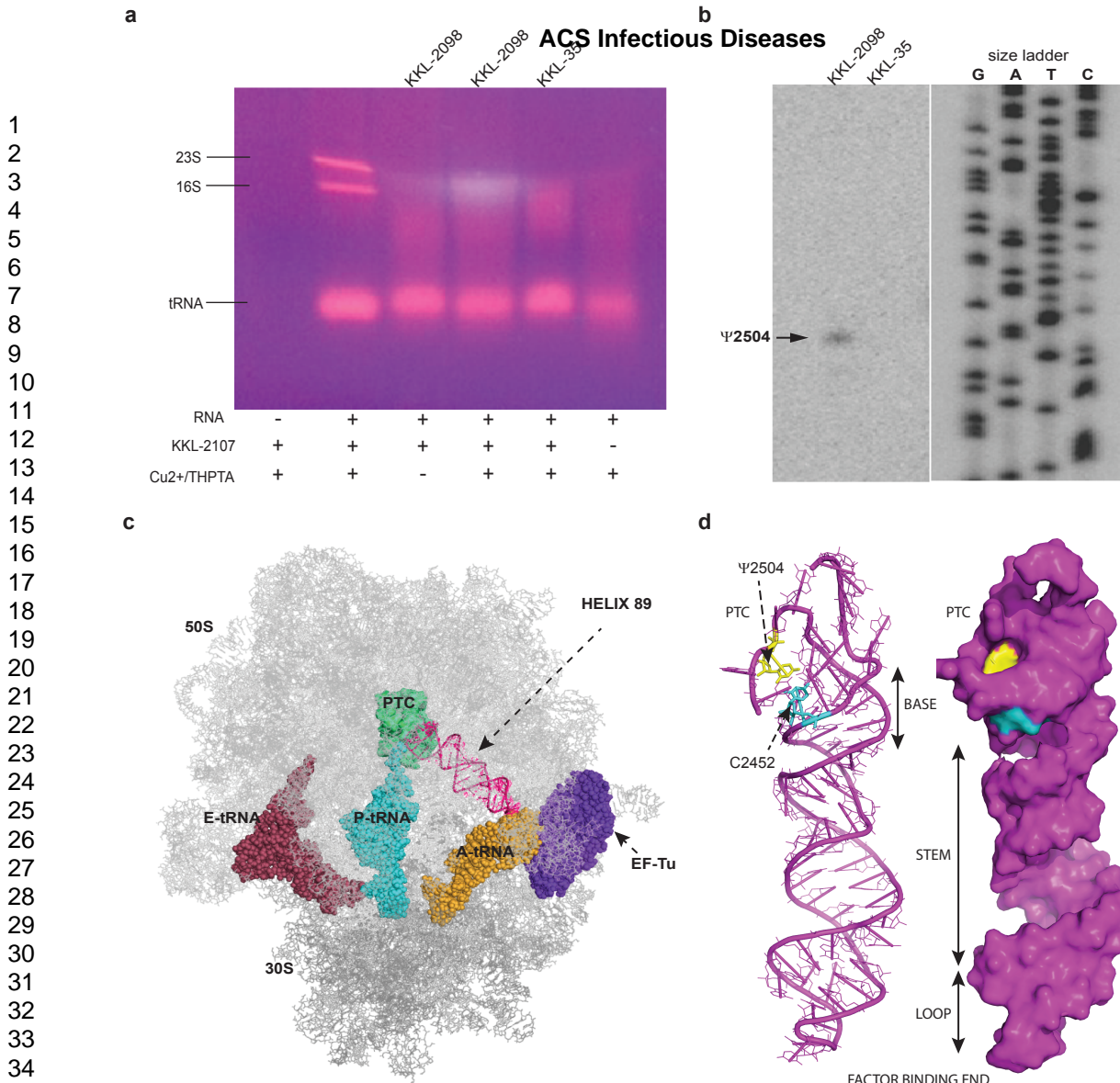
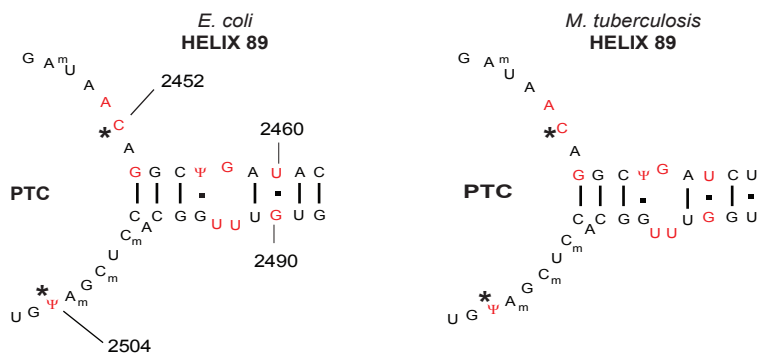


**Figure 4. KKL-2098 binds 23S rRNA.** (a) Agarose gel analysis for the click conjugation and control reactions with total RNA preparations from *M. smegmatis* cells. (b) Autoradiogram showing primer extension results using RNA prepared from cells treated with KKL-35 or KKL-2098. The arrow indicates the extension product seen only in the cross-linked sample treated with KKL-2098 (see **Fig. S3** for the full gel and experiments using other primers). (c) Structure of the *E. coli* ribosome (PDB ID 4V69) showing the location of H89 (magenta) extending from the PTC (green) to the factor binding site (purple). (d) Cartoon and surface structures of H89 showing the location of  $\Psi$ 2504 and C2452.



*E. coli*: 2450 -AACAGGCΨGAU-2460 .....2489-UGUUUGGCACCUCGAΨG - 2505  
*M. tuberculosis*: .....AACAGGCΨGAU..... GGUUUGGCACCUCGAΨG .....  
*M. smegmatis*: .....AACAGGCΨGAU..... GGUUUGGCACCUCGAΨG .....  
*B. subtilis*: .....AACAGGCΨGAU..... GGUUUGGCACCUCGAΨG .....  
*T. aquaticus*: .....AACAGGCΨGAU..... UGUUUGGCACCUCGAΨG .....

**Figure 5. Nucleotides that cross-link to KKL-2098 are highly conserved.** Comparison of the nucleotide sequence and secondary structures of H89. The KKL-2098 cross-link sites are indicated by asterisks. Mutation of the nucleotides highlighted in red is known to impair peptidyl-transferase activity, ribosome fidelity/integrity or cell growth in bacteria.<sup>24-27</sup>

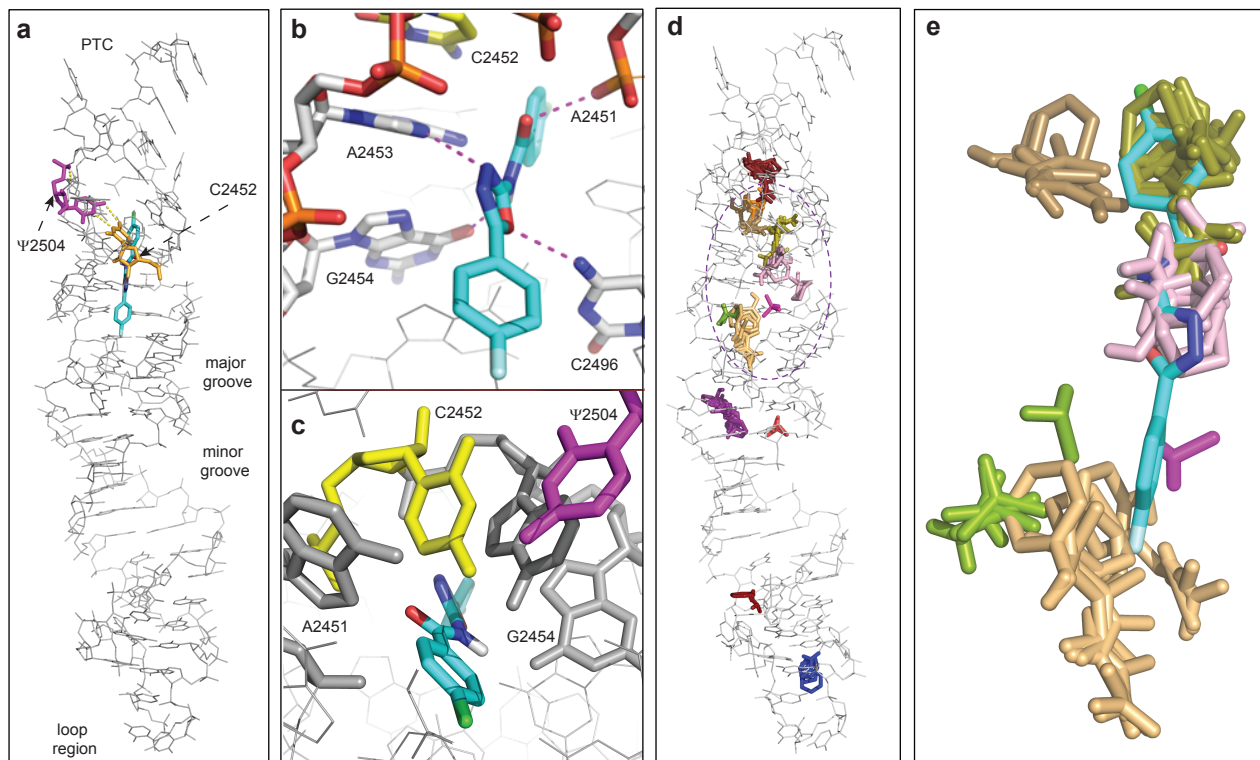
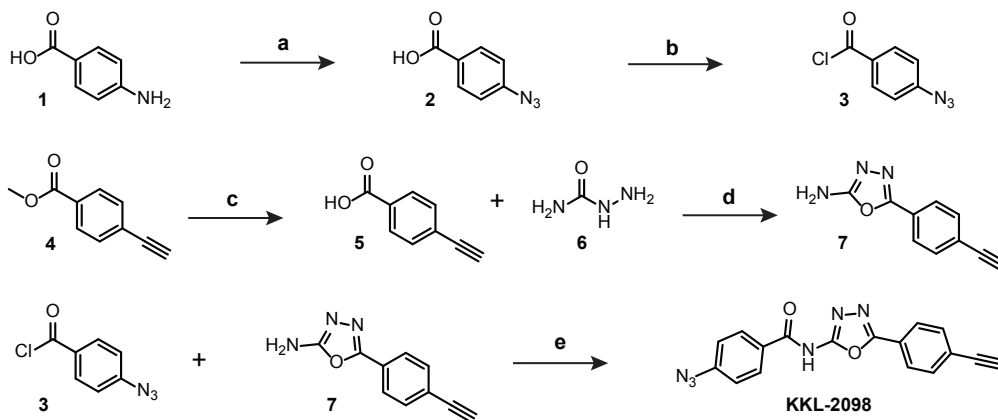


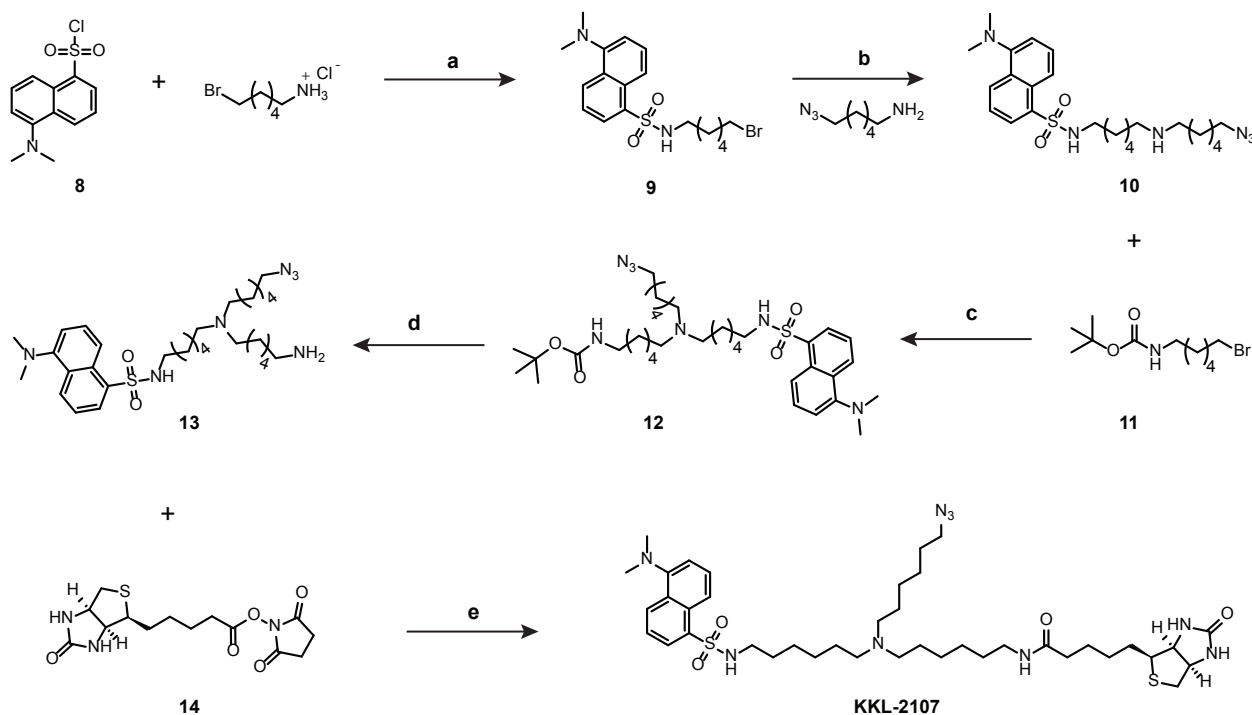
**Figure 6. KKL-35 docks to a predicted binding hot spot in H89.** (a) Docked KKL-35 (cyan) in a pocket at the base of H89 adjacent to the PTC (PDB ID 4ABR). (b) Lateral view (from the loop region) of the docking site for KKL-35 illustrating potential polar interactions (dashed lines). (c) Reversed view (from the PTC side) of the binding site (d) Solvent mapping results for H89 showing probe clustering. The dotted region indicates a hot spot located within the predicted binding site for KKL-35. (e) Close-up of the highlighted hot spot in 'd' showing the docked KKL-35 and FTMap probe clusters. Probes are color-coded to distinguish between different consensus sites (CSs): CS1-(9), CS2-(12), CS3-(11) and CS4-(4) (number of probe clusters in each CS in parenthesis).

**Scheme 1.** Synthesis of the dual function photo-reactive click probe: 4-azido-*N*-(5-(4-ethynylphenyl)-1,3,4-oxadiazol-2-yl)benzamide (**KKL-2098**)<sup>a</sup>.



<sup>a</sup>Reagent conditions: (a) NaNO<sub>2</sub>, HCl, H<sub>2</sub>O, 0 °C, 1 h; (b) NaN<sub>3</sub>, HCl, H<sub>2</sub>O, 0 °C, 1 h; (c) SOCl<sub>2</sub>, reflux 12 h; (d) NaOH, MeOH, rt, 4 h; (e) 1 N HCl, pH 2; (f) POCl<sub>3</sub>, reflux, 12 h; (g) Pyridine, 50 °C, 12 h.

**Scheme 2.** Synthesis of the tri-functional fluorescent reporter *N*-(6-((6-azidohexyl)(6-(5-(dimethyl amino) naphthalene-1-sulfonamido)hexyl)amino)hexyl)-5-((3*a*S,4*S*,6*a*R)-2-oxohexahydro-1*H*-thieno[3,4-*d*]imidazol-4-yl) pentanamide (**KKL-2107**)<sup>a</sup>.



<sup>a</sup>Reagent conditions: (a) Et<sub>3</sub>N, CH<sub>2</sub>Cl<sub>2</sub>, 0 °C - rt, rt 12 h; (b) DIPEA, CH<sub>3</sub>CN, reflux 12 h; (c) DIPEA, CH<sub>3</sub>CN, reflux 12 h; (d) TFA:CH<sub>2</sub>Cl<sub>2</sub> (1:1), 0 °C - rt, rt 3 h; (e) Et<sub>3</sub>N, MeOH, rt, 12 h.

# Ribosome Rescue Inhibitors Kill Actively Growing and Non-replicating Persister *Mycobacterium tuberculosis* Cells

John N. Alumasa,<sup>†</sup> Paulo S. Manzanillo,<sup>§</sup> Nicholas D. Peterson,<sup>¶</sup> Tricia Lundrigan,<sup>§</sup>  
Anthony D. Baughn,<sup>¶</sup> Jeffery S. Cox,<sup>§</sup> Kenneth C. Keiler.<sup>\*,†</sup>

<sup>†</sup>Department of Biochemistry and Molecular Biology, The Pennsylvania State University, University Park, PA 16802. <sup>§</sup>Department of Molecular and Cell Biology, University of California, Berkeley. CA 94720. <sup>¶</sup>Department of Microbiology and Immunology, University of Minnesota, Minneapolis, MN 55455.

